ChemPubSoc Europe

DOI: 10.1002/slct.201800035

Chemistry SELECT Full Papers

Materials Science inc. Nanomaterials & Polymers

Exploring Solvent Effects on the Dialysis-Induced Self-Assembly of Nanostructured Tetra(aniline)

Wei Lyu,[a] Mengting Yu,[a] Jiangtao Feng,*[a] and Wei Yan*[a, b]

One-pot simple dialysis process was employed to explore the self-assembly behavior of Ph/NH_2-capped tetra(aniline) (TANI) in five different solely organic solvents. Multi-morphologies of supramolecular were assembled including nanoparticles, nanocapsules, hierarchical nanoflowers and nanowires. The solvent effects on the self-assembly behavior were studied by differential scanning calorimetry (DSC), thermogravimetric analyzer (TGA), FT-IR and UV-Vis spectroscopies, ^{1}H NMR and powder X-ray diffraction (PXRD), as well as density functional theory (DFT) calculations. Investigations suggested that the increase of solvent polarity facilitated the formation of hydrogen bonding between solute-solvate. Moreover, dialysis process was found to have a profound effect on forming intermolecular π-π stacking interaction. Such results provided not only an insight into the formation mechanism and design rule of self-assembly behavior of nanostructured oligo(aniline)s in organic solvent-containing complex system, but also further understanding of dialysis-induced self-assembly system for other nanomaterials.

Introduction

Oligo(aniline)s (OANI)[1,2] based materials have become a new class of promising organic semiconductors, owing to their outstanding properties, including relatively high conductivity, unique electrochemical properties, well-defined chemical structures, good solubility and excellent processability.[3–6] The functionality of OANI-based materials are deeply related to their morphologies, such as the applications of micro/nanocapsules and vesicles for drug delivery[7–10] and nanowires in optoelectronic devices and chemical sensors.[6,11,12] Therefore, the fabrication of well-defined micro/nanostructured OANI-based functional materials is one of the most fascinating subjects of research.

Molecular self-assembly is an intriguing, controllable and low-energy approach for preparing materials with nanoscopic order.[13] Some reports have indicated that the effects of solvents are significant on molecular self-assembly. On the one hand, solvent properties, such as hydrogen bonding and polarity, can directly influence local interactions in molecular self-assembly. Wang et al.[14] discovered that solvent-bridged hydrogen bonding is a crucial force in directing the fiber formation of dipeptide molecules. Xu et al.[15] reported an unexpected solvent effect on the self-assembly of 1,7-bis-pyridinoyl perylene diimide amphiphile, where the aggregation state of amphiphile depended on the solvent polarity. On the other hand, solvent molecules can also be incorporated as part of the crystal structures in solution-driven self-assembly process. Park et al.[16] found that there is a critical correlation between the property of the solvent and the final geometry of the self-assembled C60 structure during a solution-based crystallization process.

Reports have indicated that OANI, as a class of π-conjugated molecules, can self-assemble into well-defined micro/nanostructures driven by noncovalent interactions such as π-π stacking, electrostatic interaction, hydrogen bonding and hydrophobic interaction.[3,17,18] Vertically oriented structures of OANI single crystal via π-π stacking were obtained in a binary solvent system by using graphene as a guiding substrate, where the densities and orientations can be tuned by changing solvent parameters.[11] Controlled aggregation of OANI molecules via noncovalent interactions in a variety of dopant-containing solvent systems (organic solvent and dopant acid) led to the formation of diverse structures including nanowires, nanoribbons, rectangular nanoplates and nanofibers.[6,12] Short nanofibers were also obtained via π-π stacking interaction and hydrogen bonding by a similar approach.[19] Thomas et al.[20] investigated the influence of solvent polarity on the structure of drop-cast TANI-surfactant thin films. They proposed that more polar solvents allowed the film present with greater crystallinity. However, the solvent effects on the assembled superstructures rather than on film are still unclear. And the complexity of self-assembly using binary solvent system makes it difficult to comprehend the organization mechanism. In our previous study, the self-assembly behavior of OANI in solely acidic aqueous media was investigated and the results provided insight to understand the self-assembly behavior in complex dopant-containing systems.[21] Therefore, it is necessary and desirable to understand the influence of solvent on the self-assembly of OANI nanostructures, which will

[a] Dr. W. Lyu, M. Yu, Dr. J. Feng, Prof. W. Yan
Department of Environmental Science and Engineering, Xi'an Jiaotong University, Xi'an 710049, China
Tel: +8613032912105
Fax: +86-029-82664731
E-mail: fjtes@xjtu.edu.cn
yanwei@xjtu.edu.cn
[b] Prof. W. Yan
State Key Laboratory of Multiphase Flow in Power Engineering, Xi'an Jiaotong University

Supporting information for this article is available on the WWW under https://doi.org/10.1002/slct.201800035

provide a potential formation mechanism and design rule of more complex nanostructures in organic solvent-containing system.

Dialysis was found to be a facile but powerful method for crystal engineering. Various nanostructures such as nanofiber, needle-like structure and microparticle can be fabricated via dialysis-induced self-assembly of hydrophobic pharmaceutical molecules using different organic solvents.[22] However, the effect of dialysis process on self-assembly was negligible to some extent in crystallization/precipitation and amphiphilic assembly method, where dialysis was adopted for removing the excess organic solvent. Therefore, it is desirable to uncover the dialysis-induced self-assembly behavior for OANI in different organic solvents. In this study, Ph/NH_2-capped tetra(aniline) (TANI), the shortest OANI, was selected. The dialysis-induced self-assembly behavior of TANI was investigated in five different solely organic solvents (tetrahydrofuran (THF), acetone, ethanol (EtOH), dimethylformamide (DMF) and dimethyl sulfoxide (DMSO). The dielectric constant of the solvents are listed in Table 1.

Table 1. Dielectric constant of different solvents.

Solvent	THF	Acetone	EtOH	DMF	DMSO	H_2O
Dielectric constant ε / F·m^{-1}	7.52	21.01	24.6	38.25	47	78.54

Results and discussion

Figure 1 shows the morphologies of TANI samples obtained using various organic solvents via one-pot dialysis process. Interestingly, the different superstructures of TANI molecular assembly were obtained dependent on the solvent type, indicating that solvent played the different roles in dialysis-induced self-assembly process. Spherical structure was observed for THF-TANI sample with an average diameter of 193 nm (Figure 1a,1b). The absence of the strong contrast between the pale edge and the dark center in the TEM image (Figure 1b) indicated these spherical structures were not hollow inside. Hierarchical flower superstructures with amounts of nanoparticles were observed for Acetone-TANI (Figure 1c,1d). While for EtOH-TANI, the main superstructures were nanocapsules with an average diameter of 430 nm (Figure 1e,1 f). The inner hollow of the broken one (red arrow) is the evidence for the formation of nanocapsules (Figure 1f). In the case of DMF-TANI (Figure 1g,1 h) and DMSO-TANI (Figure 1i, 1j) samples, a mixture of nanowires with average diameters of 70 nm and 60 nm, and nanoparticles with average diameters of 258 nm and 148 nm were achieved, respectively. During the dialysis process, water (a nonsolvent for TANI) gradually diffused into the inner organic phase and replaced the good solvent, leading to TANI molecules crystallization and assemble into superstructures. Although the driven force formed in a single organic solvent system is not strong enough for the formation of specific and well-defined nanostructures, the diverse of the self-assembled structures suggested that organic solvents played two different roles in forming the driven forces. In the self-assembly process, the solvent may *either* incorporate as part of the crystal structure, i.e. forming solvates *or* affect the local driven forces for TANI molecular self-assembly.

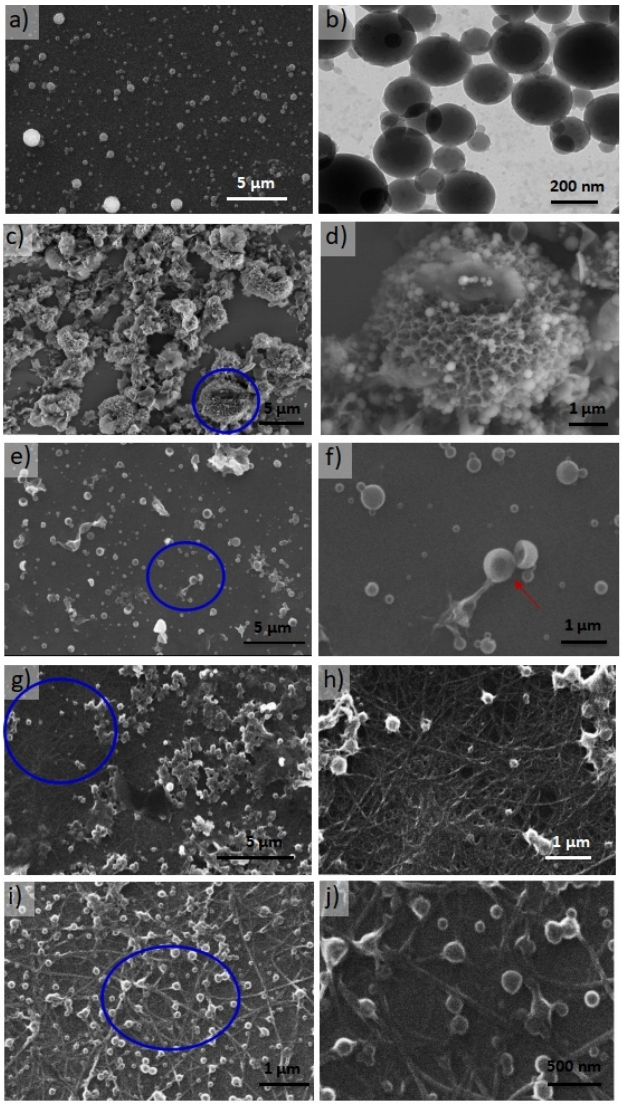

Figure 1. SEM images showing the TANI molecular assembles obtained by dialysis using various solvents: (a) THF-TANI, (c) Acetone-TANI, (e) EtOH-TANI, (g) DMF-TANI, and (i) DMSO-TANI, with TEM image of (b) THF-TANI and magnificent images of (d) Acetone-TANI, (f) EtOH-TANI, (h) DMF-TANI and (j) DMSO-TANI obtained from the indicated circular areas.

As DSC curves shown in Figure 2 inset, no endothermic peak appears in pure TANI, Acetone-TANI, EtOH-TANI, DMF-TANI and DMSO-TANI samples. While in the case of THF-TANI sample, a peak located at around 108 °C was observed, indicating the presence of solvate resulting from THF in final nanocapsules. TGA curves shown in Figure 2 further verify the existence of the solvate. Weight loss occurred at approximately 81 °C in the range of 30–300 °C was observed for THF-TANI sample, while no obvious weight loss occurred for the others

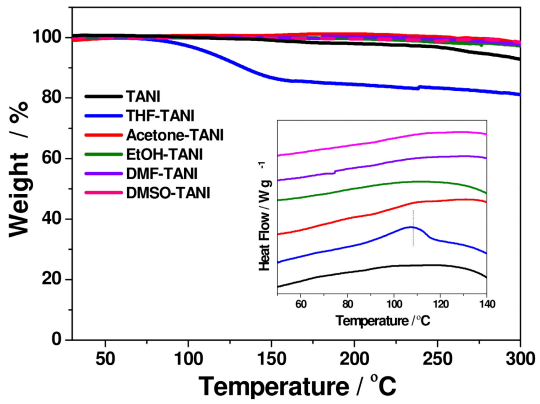

Figure 2. TGA and DSC (inset) curves of different samples.

within this range. Besides, it has no weight loss at 66 °C (boiling point of THF), which indicated that in the dialysis-induced self-assembly of TANI molecule, solvate would be formed from THF and incorporated as part of the TANI superstructure.[22]

As shown in FT-IR spectra from 1800 to 1200 cm^{-1} (Figure 3), the characteristic vibrations of all samples are located at

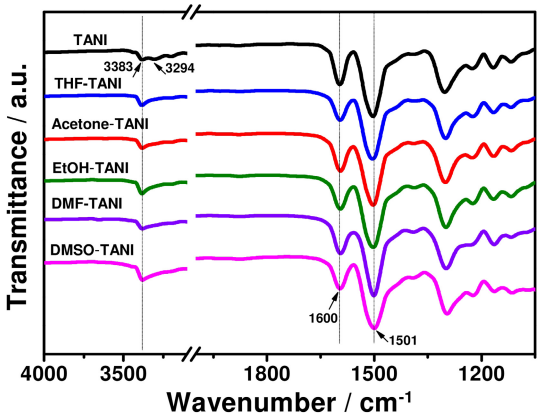

Figure 3. Pellet (KBr) FT-IR spectra of different samples.

1600 cm^{-1} (νC=C for quinoid rings) and 1501 cm^{-1}(νC=C for benzenoid rings), which are typical for TANI-EB state. It is well-known that a hydrogen-bonded N–H bond between amine and imine exists in TANI-EB state.[23] In Figure 3, the peak of this hydrogen bond located around 3294 cm^{-1} in as-synthesized TANI-EB sample. However, this peak disappeared completely in all of the dialyzed samples, suggesting that the hydrogen bonding in the oligomer chains (N···H···N) in TANI powder was disrupted by these five solvents and no new strong hydrogen-bonded N–H bond generated during the dialysis process. Besides, no shift occurred for the peaks at 3383 cm^{-1} attributed to the free N–H stretch for all samples,[23] indicating that the difference of N–H hydrogen bonding interaction was very slight at least in our FT-IR experimental.

^{1}H NMR measurements in different deuterated solvents were therefore carried out to further study the differences of N–H hydrogen bonding in these solvents. However, as Irena Kulszewicz-Bajer et al.[1] stated that oxidation of TANI using the traditional oxidative coupling method can lead to different positional isomers of Ph/NH_2 TANI (Scheme 1), ^{1}H NMR spectra

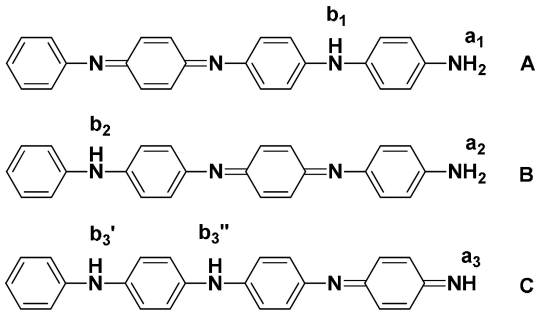

Scheme 1. Three positional isomers of Ph/NH_2 TANI in EB state (A,B,C).

of TANI-EB with poor intensity in different deuterated solvents were always obtained (Figure S2). Fortunately, the signals of amine group in these solvents can be distinguished, which provided the information of solvent effects on the active protons. As shown in Table 2, two signals at 4.03 and 4.85 ppm

Table 2. ^{1}H-NMR data of terminal NH_2 group protons in TANI-EB.

Deuterated solvents	TANI-EB $NH_2(a_1)$ / ppm	$NH_2(a_2)$ / ppm
THF-d_8	4.03	4.85
Acetone-d_6	4.37	4.97
Ethanol-d_6	4.63	/
DMF-d_7	4.73	5.49
DMSO-d_6	4.76	5.54

attributed to the NH_2 protons of the groups located further and closer to the quinoid ring, i.e., iosmoers A and B, were observed for TANI-EB in THF-d_8 solvent. These signals for the corresponding resonance appeared at 4.37 and 4.97 ppm for TANI-EB in Acetone-d_6, 4.73 and 5.49 ppm in DMSO-d_8 and 4.76 and 5.54 ppm in DMF-d_7, respectively. For Ethanol-d_6 solvent, the solubility of TANI is lower than the others, so only one strong signal of terminal NH_2 group protons located at 4.63 ppm was observed, suggesting the TANI molecule in the form of isomer A has a higher solubility than isomer B in Ethanol-d_6 solvent. Nevertheless, it could be concluded that the signal of terminal NH_2 group protons was downfield shifted with the increase of solvent polarity (from 4.03 ppm in THF-d_8 to 4.76 ppm in DMF-d_7 for isomer A), indicating a possible increase in the extent of hydrogen bonding in the solvent.[24,25]

Preliminary theoretical computational work was carried out to explore solvent effects on TANI molecular assembly. Bond-length alternation parameter (BLA) for the molecular fragments shown in Figure 4 was firstly selected to study the medium effects on the molecular geometry of TANI. The BLA calculation

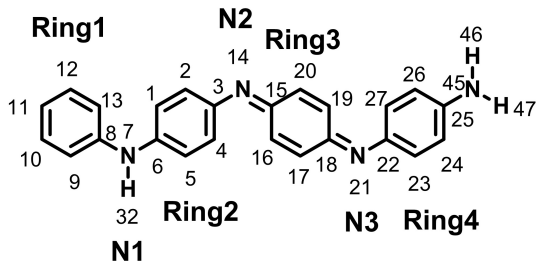

Figure 4. Scheme showing the fragments of TANI.

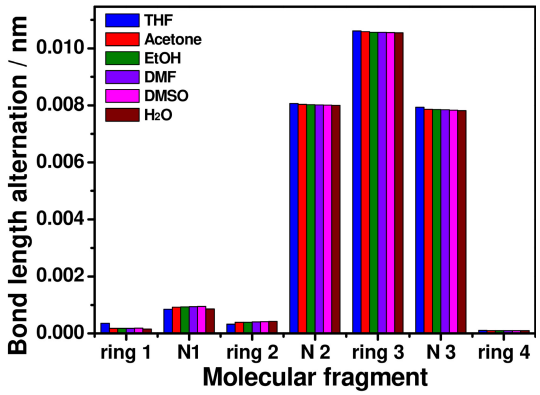

Figure 5. BLA values of optimized TANI molecular fragment in various solvents (B3LYP/6-31G (d, p)/PCM).

for the ring fragments is the subtraction of the averaged "single" C–C bonds from the averaged "double" C–C bonds.[26] As shown in Figure 5, although the difference in the BLA values of optimized structures in different solvents is not obvious, it still could be noted that the BLA value for N2, Ring3 and N3 molecular fragments decreased with the increase of solvent polarity, which may result in the change of imine N atomic charge (N14 and N21).

Table 3 shows the natural bond orbital (NBO) charges of each fragment in different solvents calculated using BLYP / 6–31 G (d, p) / PCM method. We observe that the solvent polarity has a noticeable effect on the NBO charges of quinoid ring fragment, i.e. N14, ring3 and N21. With the increase of solvent polarity, the electronegativity of imine N (N14 and N21) in TANI molecule increases (from −0.44027 and −0.43434 in THF solvent to −0.44609 and −0.43941 in H_2O, respectively). This indicated that the chance for forming hydrogen bonding

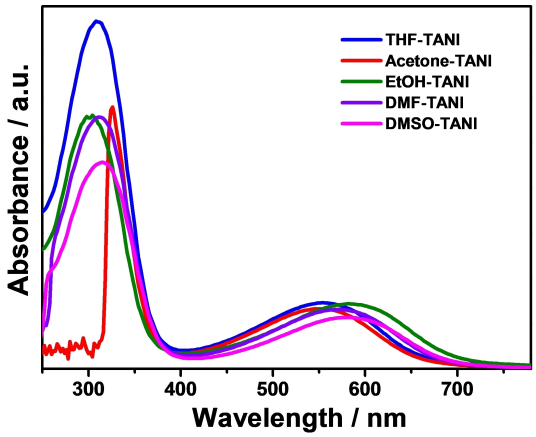

Figure 6. Normalized UV-Vis spectra of as-synthesized TANI dissolved in five different organic solvents.

between TANI molecule and solvent molecule increased, which would drive TANI molecule self-assemble into well-defined micro/nanostructures. Besides, the raise of solvent polarity enhanced the solvation effect on TANI molecule where the dipole moment (μ) increases from 2.7751 D in THF to 2.9521 D in H_2O, which was supported by the previous ^{1}H NMR discussions.

However, comparing with the morphologies obtained using the different solvents (Figure 1), we notice that 3-D hierarchical flowers appear in the acetone dialyzed system, while THF, EtOH, DMF, DMSO lead to nanofibers and hollow spheres, the small difference in solvent effects such as hydrogen bonding alone do not appear sufficient to make a big difference in these superstructures. Therefore, UV-Vis spectra of the dissolved samples were obtained to further investigate the solvatochromism effect. As shown in Figure 6, the peak around 300 nm assigned to the π-π* transition was observed in EtOH. This peak red shifted to ~310 nm in THF, DMF and DMSO, while in acetone the transition was moved to the higher wavelength of ~325 nm. The red shift often results from a rather distorted π-π stacking allowing the exitionic transitions in lower energy. [12] On the other hands, the peak located at ~580 nm is attributed to the π-polaron band transition for typical TANI-EB.[27] In EtOH and DMSO, this peak red shifted to ~590 nm, while in DMF the transition blue shifted to ~570 nm and the transition in acetone or THF further moved to the lower wavelength of ~550 nm. This transition at a longer wavelength corresponds to a better π-π stacking and a more extended chain

Table 3. NBO charges and dipole moment of TANI in different solvents.

Solvent	Ring 1	Ring2	N14	Ring3	N21	Ring4	μ/ D
THF	0.10806	0.25396	-0.44027	0.45263	-0.43434	-0.00349	2.7751
Acetone	0.10829	0.2537	-0.4442	0.45125	-0.43776	0.00146	2.8976
EtOH	0.10831	0.25367	-0.44463	0.45111	-0.43813	0.002	2.9116
DMF	0.10833	0.25363	-0.44531	0.45086	-0.43872	0.00286	2.9334
DMSO	0.10835	0.2536	-0.44562	0.45069	-0.43897	0.00328	2.9425
H_2O	0.10845	0.25354	-0.44609	0.45047	-0.43941	0.00391	2.9521

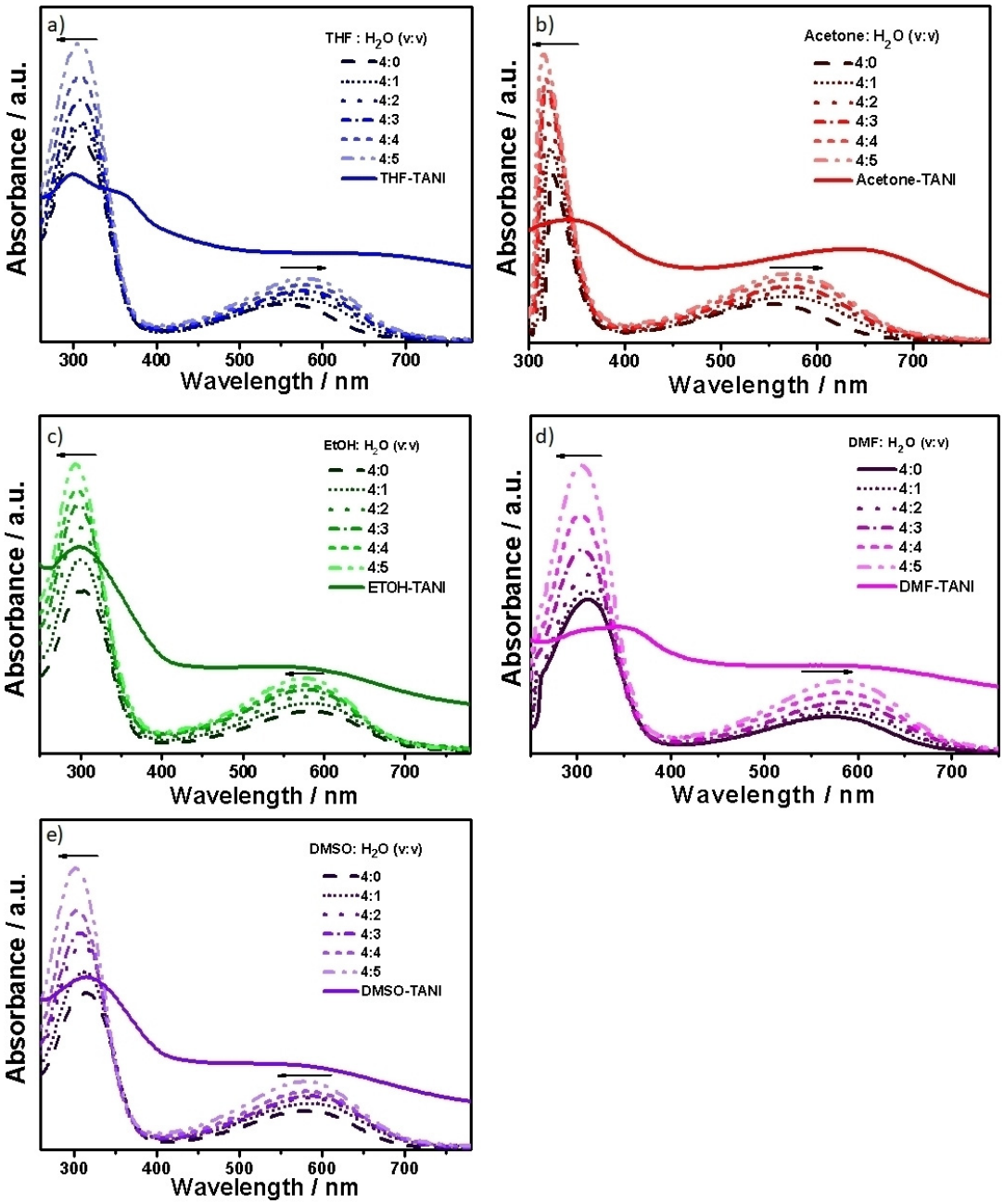

Figure 7. UV-Vis spectra of TANI-EB in different ratio of organic solvents and water mixture (dotted line), and the obtained dispersion after dialysis (solid line).

conformation.[28] The obtained results were similar to those in Wang's study of solvatochromism effects on TANI molecule.[12] However, both of the results were inconsistent with the self-assembled superstructures: TANI molecules intended to self-assemble into well-defined structures with higher π-π stacking interaction in EtOH, DMF and DMSO solvents, while random structures were likely to occur in acetone, instead of being nanoflowers. A likely explanation is that the effect of dialysis process may be neglectable, i.e. the slowly diffusion of water into the dialysis bag made the system a mixture of organic solvent and water rather than the pure organic solvent.

Hence, UV-Vis measurements of different ratio of different organic solvent and water and the obtained dialyzed dispersions were carried out. Different amounts of water were added to the certain system (0.5 mg TANI/mL solvent) to simulate the dialysis system. Interestingly, we got the different results compared with the one dissolved in pure organic solvents. As shown in Figure 7, the π-π* transition moved to a lower wavelength in all five solvents with an increase amount of water, indicating that TANI molecules started to self-assemble driven by intermolecular interactions at the very beginning of dialysis. Moreover, for THF (Figure 7a), Acetone (Figure 7b), and DMF (Figure 7d), the π-polaron band transition moved to a

higher wavelength with an increase amount of water, suggesting that TANI molecules in these systems tended to exhibit a more extended chain conformation than the ones in EtOH and DMSO system. Besides, this transition located at around 641 nm in the UV-Vis spectra of the obtained Acetone-TANI dispersion indicated that a strong π-π stacking interaction existed in the self-assembled structures. This was well agreed with the appearance of hierarchical nanoflower structures shown in Figure 1.

Besides, PXRD of Acetone-TANI sample had well-defined peaks compared with other samples (Figure 8), indicating that

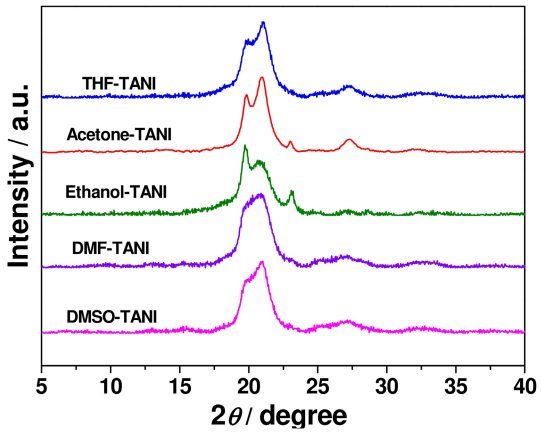

Figure 8. X-ray diffraction patterns of the obtained samples.

the nanostructures showed crystallinity in this sample[29] and it further supported the above discussions in UV-Vis analysis and SEM observations. In terms of another four samples, all of them presented weaker band intensity of π-polaron band transition and poor-defined peaks in PXRD, which were consistence with their morphologies. Therefore, we can conclude that dialysis was not only a simple purification process, the dialysis-induced changes of composition between the organic solvent and water but also played the crucial role in the formation of nanostructures' self-assembly. The inherent causes of mixed solvents effects i.e. the driven forces, are under investigation.

Conclusions

We have shown the assembly behaviour of TANI in solely organic solvent via a facile dialysis process. Different micro/nanostructures were fabricated dependent on the employed solvents. Studies of DLS and TGA measurements showed that THF solvent tended to form solvates with TANI during the assembly process. ^{1}H NMR and DFT theoretical calculation on solvent effects indicated that TANI molecules have the tendency to self-assemble into well-defined structures in organic solvent with high polarity, due to the higher probability of forming hydrogen bonding between solute-solvate. The UV-Vis spectra results suggested that dialysis process played a profound effect on the final structures, where TANI molecules existed different chain conformations in the solvent mixtures compared with the ones in solely organic solvents. Moreover, combining with PXRD results, we can conclude that more extended chain conformations of TANI existed in the acetone dialyzed system. These results provided preliminary insight to formation mechanism and design rule of nanostructured OANI in complex organic solvent-containing systems involved in dialysis process, as well as a new understanding for dialysis-induced self-assembly system for other nanomaterials.

Supporting Information Summary

Full experimental details including synthetic route, self-assembly process, and characterization, full computational details and results, and the ^{1}H NMR spectra of TANI-EB in different deuterated solvents are available in the Supporting Information.

Acknowledgment

The authors gratefully acknowledge the National Science and Technology Support Program (No. 2015BAD16B03).

Conflict of Interest

The authors declare no conflict of interest.

Keywords: dialysis · nanostructures · self-assembly · solvent effects · tetra(aniline)

[1] I. Kulszewicz-Bajer, I. Rozalska, M. Kurylek, *New J. Chem.* **2004**, *28*, 669–675.
[2] I. Rozalska, P. Kulyk, I. Kulszewicz-Bajer, *New J. Chem.* **2004**, *28*, 1235–1243.
[3] Z. Shao, Z. Yu, J. Hu, S. Chandrasekaran, D. M. Lindsay, Z. Wei, C. F. J. Faul, *J. Mater. Chem.* **2012**, *22*, 16230–16234.
[4] Z. Wei, C. F. J. Faul, *Macromol. Rapid Commun.* **2008**, *29*, 280–292.
[5] C. U. Udeh, N. Fey, C. F. J. Faul, *J. Mater. Chem.* **2011**, *21*, 18137–18153.
[6] Y. Wang, H. D. Tran, L. Liao, X. Duan, R. B. Kaner, *J. Am. Chem. Soc.* **2010**, *132*, 10365–10373.
[7] H. Kim, S. M. Jeong, J. W. Park, *J. Am. Chem. Soc.* **2011**, *133*, 5206–5209.
[8] Z. Yang, X. Wang, Y. Yang, Y. Liao, Y. Wei, X. Xie, *Langmuir* **2010**, *26*, 9386–9392.
[9] Y. Wu, S. Liu, Y. Tao, C. Ma, Y. Zhang, J. Xu, Y. Wei, *ACS. Appl. Mater. Interfaces* **2014**, *6*, 1470–1480.
[10] Q. Chen, X. Yu, Z. Pei, Y. Yang, Y. Wei, Y. Ji, *Chem. Sci.* **2017**, *8*, 724–733.
[11] Y. Wang, J. A. Torres, A. Z. Stieg, S. Jiang, M. T. Yeung, Y. Rubin, S. Chaudhuri, X. Duan, R. B. Kaner, *ACS Nano* **2015**, *9*, 9486–9496.
[12] Y. Wang, J. Liu, H. D. Tran, M. Mecklenburg, X. N. Guan, A. Z. Stieg, B. C. Regan, D. C. Martin, R. B. Kaner, *J. Am. Chem. Soc.* **2012**, *134*, 9251–9262.
[13] T. Aida, E. W. Meijer, S. I. Stupp, *Science* **2012**, *335*, 813–817.
[14] J. Wang, K. Liu, L. Yan, A. Wang, S. Bai, X. Yan, *ACS Nano* **2016**, *10*, 2138–2143.
[15] S. Xu, J. Sun, D. Ke, G. Song, W. Zhang, C. Zhan, *J. Colloid Interf. Sci.* **2010**, *349*, 142–147.
[16] C. Park, H. J. Song, H. C. Choi, *Chem. Commun.* **2009**, 4803–4805.
[17] Y. Zhao, E. Tomšík, J. Wang, Z. Morávková, A. Zhigunov, J. Stejskal, M. Trchová, *Chem. Asian J.* **2013**, *8*, 129–137.
[18] Y. Zhao, J. Stejskal, J. Wang, *Nanoscale* **2013**, *5*, 2620–2626.
[19] Y. Li, W. He, J. Feng, X. Jing, Self-assembly of aniline oligomers in aqueous medium, *Colloid Polym. Sci.* **2012**, *290*, 817–828.

[20] T. G. Dane, J. E. Bartenstein, B. Sironi, B. M. Mills, O. Alexander Bell, J. Emyr Macdonald, T. Arnold, C. F. J. Faul, W. H. Briscoe, *Phys. Chem. Chem. Phys.* **2016**, *18*, 24498–24505.
[21] W. Lyu, J. Feng, W. Yan, C. F. J. Faul, *J. Mater. Chem.C* **2015**, *3*, 11945–11952.
[22] Y. Dou, Y. Jia, X. Zhou, J. Zhang, X. Li, *Cryst. Growth Des.* **2011**, *11*, 899–904.
[23] W. Zheng, M. Angelopoulos, A. J. Epstein, A. G. MacDiarmid, *Macromolecules* **1997**, *30*, 2953–2955.
[24] T. P. Pitner, D. W. Urry, *J. Am. Chem. Soc.* **1972**, *94*, 1399–1400.
[25] M. Iqbal, P. Balaram, *Biopolymers* **1982**, *21*, 1427–1433.
[26] J. Romanova, G. Madjarova, A. Tadjer, N. Gospodinova, *Int. J. Quantum Chem.* **2011**, *111*, 435–443.
[27] Z. Shao, P. Rannou, S. Sadki, N. Fey, D. M. Lindsay, C. F. Faul, *Chem. Eur. J.* **2011**, *17*, 12512–12521.
[28] W. Lv, J. Feng, W. Yan, C. F. J. Faul, *J. Mater. Chem. B* **2014**, *2*, 4720–4725.
[29] J. P. Pouget, M. E. Jozefowicz, A. J. Epstein, X. Tang, A. G. MacDiarmid, *Macromolecules* **1991**, *24*,779-789.

Submitted: January 4, 2018
Revised: March 12, 2018
Accepted: March 14, 2018